Improvement of the energy and exergy efficiencies of the parabolic solar collector equipped with a twisted turbulator using SWCNT-Cu/water two-phase hybrid nanofluid

Muhammad Ibrahim [a,g,*], Awatef Abidi [b,c,d], Ebrahem A. Algehyne [e,f], Tareq Saeed [g], Goshtasp Cheraghian [h], Mohsen Sharifpur [i,j,*]

[a] Department of Basic Sciences and Humanities, CECOS University of IT and Emerging Sciences, Peshawar, Pakistan
[b] Physics Department, College of Sciences Abha, King Khalid University, Saudi Arabia
[c] Research Laboratory of Metrology and Energetic Systems, National Engineering School, Energy Engineering Department, Monastir University, Monastir City, Tunisia
[d] Higher school of Sciences and Technology of Hammam Sousse, Sousse University, Tunisia
[e] Department of Mathematics, Faculty of Science, University of Tabuk, P.O.Box741, Tabuk 71491, Saudi Arabia
[f] Nanotechnology Research Unit (NRU), University of Tabuk, Tabuk 71491, Saudi Arabia
[g] Nonlinear Analysis and Applied Mathematics (NAAM)-Research Group, Department of Mathematics, Faculty of Science, King Abdulaziz University, P.O. Box 80203, Jeddah 21589, Saudi Arabia
[h] Technische Universität Braunschweig, 38106 Braunschweig, Germany
[i] Department of Mechanical and Aeronautical Engineering, University of Pretoria, South Africa
[j] Department of Medical Research, China Medical University Hospital, China Medical University, Taichung, Taiwan

ARTICLE INFO

Keywords:
Twisted turbulators
Solar collector
Numerical simulation
Two-phase flow
Exergy and energy efficiency
SIMPLEC

ABSTRACT

In the present numerical study, the effect of twisted turbulator on the improvement of energy and exergy efficiencies and hydraulic performance of SWCNT-Cu/water hybrid nanofluid in a solar collector is evaluated using computational fluid dynamics and ANSYS-FLUENT software. In this study, SOLIDWORKS software is employed to draw the geometry of the solar collector. Since the fluid flow in the solar collector is turbulent, the SST $k-\omega$ turbulence model is used. In addition, a mixed two-phase model is employed to model the hybrid nanofluid. The study is performed for Reynolds numbers (Re) in the range of 9000 to 36000, volume fractions (φ) of 1 to 3%, and turbulator pitch ratios (PR) of 1, 2, 3, and 4. It can be concluded that the average Nusselt number and the pressure drop are ascending functions of φ and Re. Also, the amount of pressure drop and the average Nusselt number is enhanced with the PR. At φ = 3% and Re = 36,000, the twisted turbulator with PR = 4 intensifies the average Nusselt number by 74.95% compared to the solar collector without turbulator. At φ = 3% and Re = 36,000, the twisted turbulator with PR = 4 enhances the pressure drop by 429.31% compared to the solar collector without turbulator. In a solar collector with a twisted turbulator with PR = 4 and φ = 3%, the amount of energy efficiency is enhanced by 41.75% by enhancing the Re from 9000 to 36000. In a solar collector with a turbulator with PR = 1 and φ = 3%, the amount of exergy efficiency is enhanced by 33.09% by intensifying the Re from 9000 to 36000.

Introduction

Today, the optimal use of energy [1–7], especially renewable energy [8–10], is an important issue due to the energy management demand [11,12,53] and increasing energy consumption. Improvement of the solar collector (SC) performance can be helpful in encouraging people to use them. In recent decades, several methods have been developed to improve heat transfer in various systems, such as microchannel [13–15], and many researchers have used these methods to improve their performance and enhance their efficiency. According to open literature, nanofluids may enhance heat transfer [16–23,55] because of their superior thermal properties to the base fluids [24–30,54,56]. Hong et al. [31] numerically examined the impact of water-copper nanofluid on the thermal performance of a parabolic SC using the finite volume method and FLUENT software. They used SOLIDWORKS software to design the geometry of PSC. They also used the SIMPLE algorithm to discretize the

* Corresponding authors at: Department of Mechanical and Aeronautical Engineering, University of Pretoria, South Africa (M. Sharifpur).
E-mail addresses: muhammad.ibrahim@cecos.edu.pk (M. Ibrahim), mohsen.sharifpur@up.ac.za (M. Sharifpur).

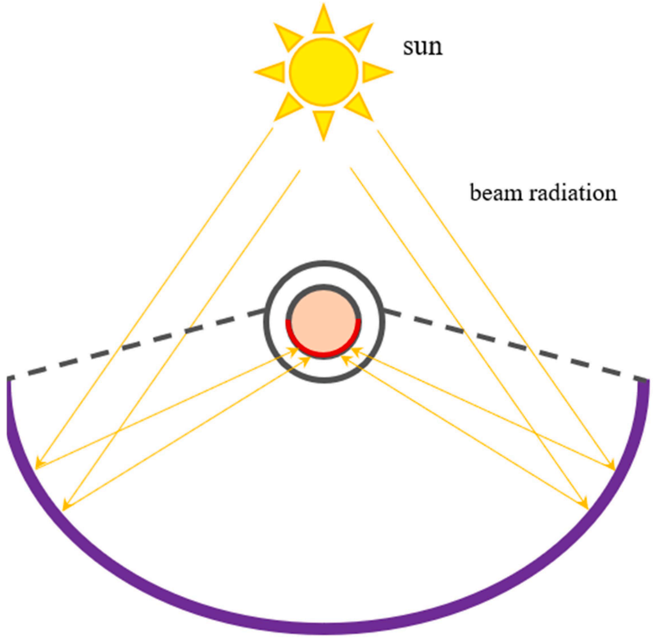

Fig. 1. Schematic of SC.

governing equations. The results demonstrated that the use of water-copper nanofluid significantly improves PSC effectiveness. Also, the thermal performance of SC is enhanced significantly by intensifying the φ.

Alimoradi et al. [32] inspected SC thermal response in the presence of turultor channel under constant heat flux experimentally and numerically using FLUENT software for numerical simulations. They employed modeler design software to design the geometry. Based on the results reported by the authors, the experimental and numerical data were in good agreement with each other. An increment in the Re and the PR of the twisted turbulator (TT) resulted in an improvement in heat transfer. In addition, the use of holes in TTs enhances heat transfer and reduces pressure drop in the cavity.

Dezfulizadeh et al. [33] used the finite volume method and FLUENT

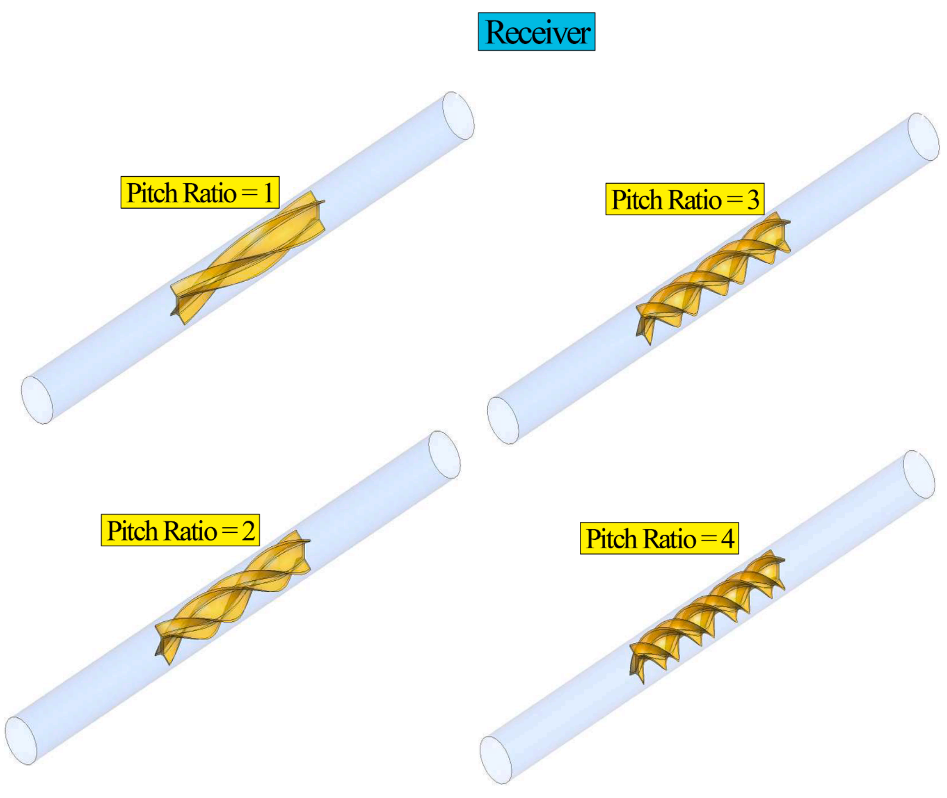

Fig. 2. Schematic of the receiver tube equipped with a TT with different values of PR.

Table 1
Thermophysical properties of base fluid and nanoparticles (298 K) [33,47].

Property	Water	Cu	SWCNT
$\rho(kg.m^{-3})$	998.2	8954	1047
$c_P(J.kg^{-1}.K^{-1})$	4182	383	3428
$k(W.m^{-1}.K^{-1})$	0.6	400	0.6833
$\mu(kg.m^{-1}.s^{-1})$	0.001003	–	–

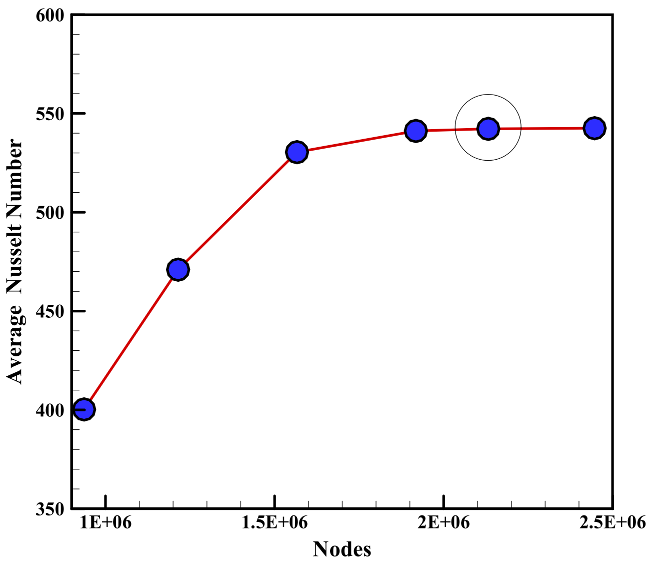

Fig. 3. Grid independence results in terms of the $\overline{Nu}$ for SWCNT-Cu/water two−phasehybridnanofluid in SC with TT for Re = 36000, φ = 3%, and PR = 4.

software to examine the effect of grooved turbulators under the influence of a magnetic field on the exergy efficiency of a heat exchanger. They used a hybridnanofluid combined with three nanoparticles and demonstrated that the exergy efficiency is enhanced by enhancing the φ and Re.

Wu et al. [34] numerically examined the effect of absorbent tubes and different directions within the parabolic SC using the finite volume method and FLUENT software. They employed the SIMPLE algorithm to discretize the equations. It was found that the use of absorber tubes with a slope of 3° leads to the maximum thermal performance of the parabolic solar collector (PSC).

Ebrahimpour and Sheikholelami [35] numerically studied the effect

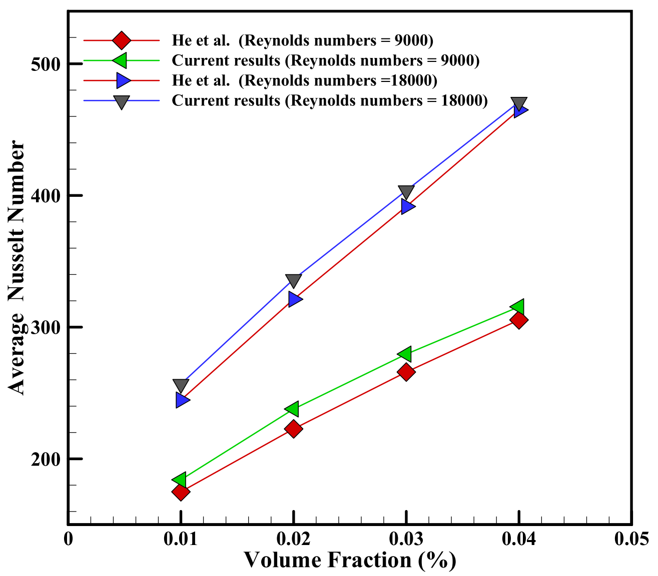

Fig. 4. Validation of the present numerical simulation with the results of He et al. [52]

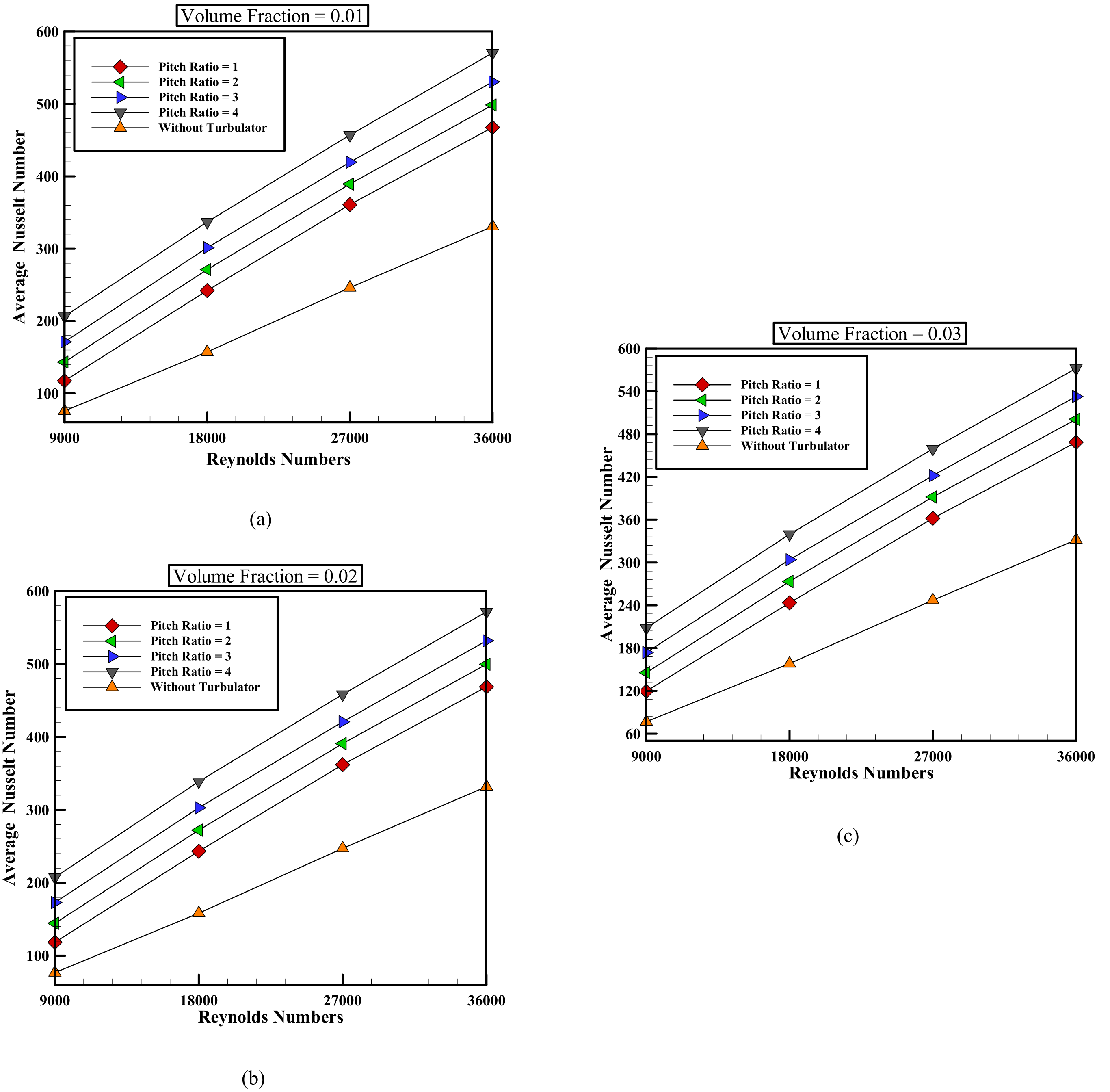

Fig. 5. The $\overline{Nu}$ versus Re in a SC equipped with a TT with different values of PR for (a) φ = 1%, (b) φ = 2%, and (c) φ = 3%.

of different angles of a SC mirror filled with nanofluid. They also used the finite volume method and FLUENT software for the simulations. The results revealed that an increment in the angle of the SC mirrors and an enhancement in the Re intensify SC thermal response. The SC usefulness was improved up to 65.23% by changing the angle of the mirrors.

The exergy analysis was also used in many studies [36,37]. Nazir et al. [38] investigated the effect of Al_2O_3/water on the exergy and energy efficiency of a SC in a laminar flow regime. They also evaluated the effect of φ and demonstrated that there is a linear relationship between exergy and energy efficiency with the φ so that the exergy and energy efficiency is improved with the φ.

Akbarzadeh and Valipour [39] inspected the first/second laws sensitivity to helical turbulator using the finite volume method and ANSYS FLUENT software. They focused on the effect of different values of PR in the helical turbulator on the energy and exergy efficiencies of the SC. It was found that the use of a helical turbulator significantly enhances the exergy and energy efficiency compared to a simple SC. In addition, the exergy efficiency was reduced with the PR.

Ma et al. [40] inspected TTs efficacy in the space between a cylinder filled with copper/water-EG. The flow regime was turbulent, and the $k-\varepsilon$ turbulence was employed along with SIMPLE approaches According to the results reported by the authors, due to the nanofluid flow through the twisted tubes, the disturbance is generated in the viscous sublayer, resulting in an enhancement in the average Nusselt number ($\overline{Nu}$).

Chang et al. [41] investigated the effect of twisted tapes on the thermal performance of PSCs. Their study was performed for different values of Re 7000 to 30,000 in. They used the standard k-ε turbulence.

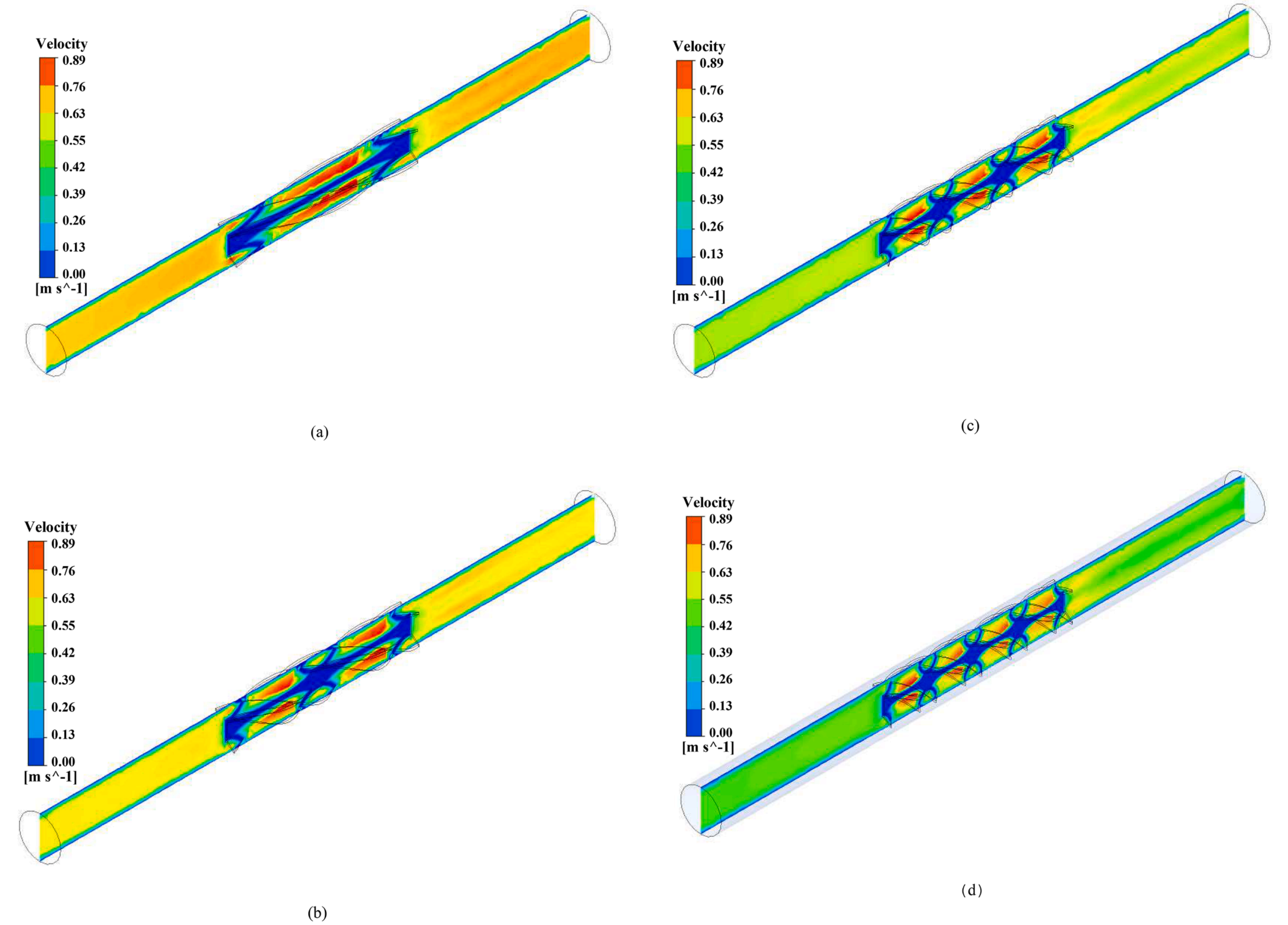

Fig. 6. 6. Velocity contours for two −phasehybridnanofluid with φ = 3% and Re = 36000 are shown in Fig. 6 for (a) PR = 1, (b) PR = 2, (c) PR = 3, and (d) PR = 4.

Their results demonstrated that placing the twisted tape and enhancing its PR results in an improvement in heat transfer (HT) in the PSC. Also, the maximum HT rate in the PSC was improved by 187.90% at Re = 30,000.

Mashayekhi et al. [42] used the finite volume method and FLUENT software to evaluate the effect of different values of PR of spiral turbulator on thermal −hydraulicperformance(THP) of two-phase water-silver nanofluid in a channel. They considered φ = zero to 4% and the different values of PR of the helical turbulator in the range of Re from 100 to 1500. It can be concluded that the placement of the helical turbulator and enhancement of its pitch ratio enhances the THP of the channel. In addition, the amount of HT is enhanced with the φ in a water/silver nanofluid.

Siavashi et al. [43] inspected the THP sensitivity of two −phasewater −aluminumnanofluid in a channel by utilizing k-ω turbulence two-phase model. The results revealed that the placement of porous ribs and an increment in their height have a significant effect on enhancing the rate of HT. Also, the use of two-phase water-aluminum oxide nanofluid experienced better THP than water-based fluid.

Goldanlou et al. [44] examined PSC effectiveness filled with hybridnanofluid using the finite volume method and FLUENT software. They used design modeler software to model the geometry of the PSC. They employed the k-ε turbulence model for their simulations. It was shown that the use of a hybrid nanofluid improves the thermal performance of the PSC compared to the base fluid.

Abbasi Varzeneh et al. [45] employed computational fluid dynamics to examine the effect of rib height on the THP of water/aluminum oxide nanofluid in a heat exchanger. The aim of this study was to investigate the impact of different heights of triangular ribs in the turbulent flow regime at Re = 5000–20,000. They demonstrated that an increment in the height of the triangular ribs enhances the $\overline{Nu}$ and reduces the pressure drop. In addition, the maximum improvement of 67.21% in thermal performance of the heat exchanger corresponded to the rib with a height of 12 mm and Re = 20,000.

Rostami et al. [46] added elliptical tubes to a SC filled with nanofluid. They used water/multi-walled carbon nanotubes as working fluid. They inspected the impact of the φ and Re on SC performance. The authors showed that the exergy efficiency is an ascending function with Re and φ.

According to the studies performed so far, the effect of a TT on THP, exergy and energy efficiency of two-phase SWCNT-Cu/water hybrid nanofluid inside a SC was not examined. Hence, in this numerical study, the effect of two-phase SWCNT −Cu/waterhybridnanofluid at $\varphi = 1$ to 3%, Re = 9000–36000, and PR = 1, 2, 3, and 4 are examined. The use of new geometry in turbolator design is the most important innovation of this study. On the other hand, the use of polymer hybrid nanofluids in parabolic collectors is another innovation of this research.

Geometric model and formulation

The geometry of the SC is shown schematically in Fig. 1.

Figure 2 illustrates a schematic of a receiver tube equipped with a TT at different values of PR. The length of the absorber tube is 900 mm and the length of the TT is 350 mm. Also, the distance between the turbulator

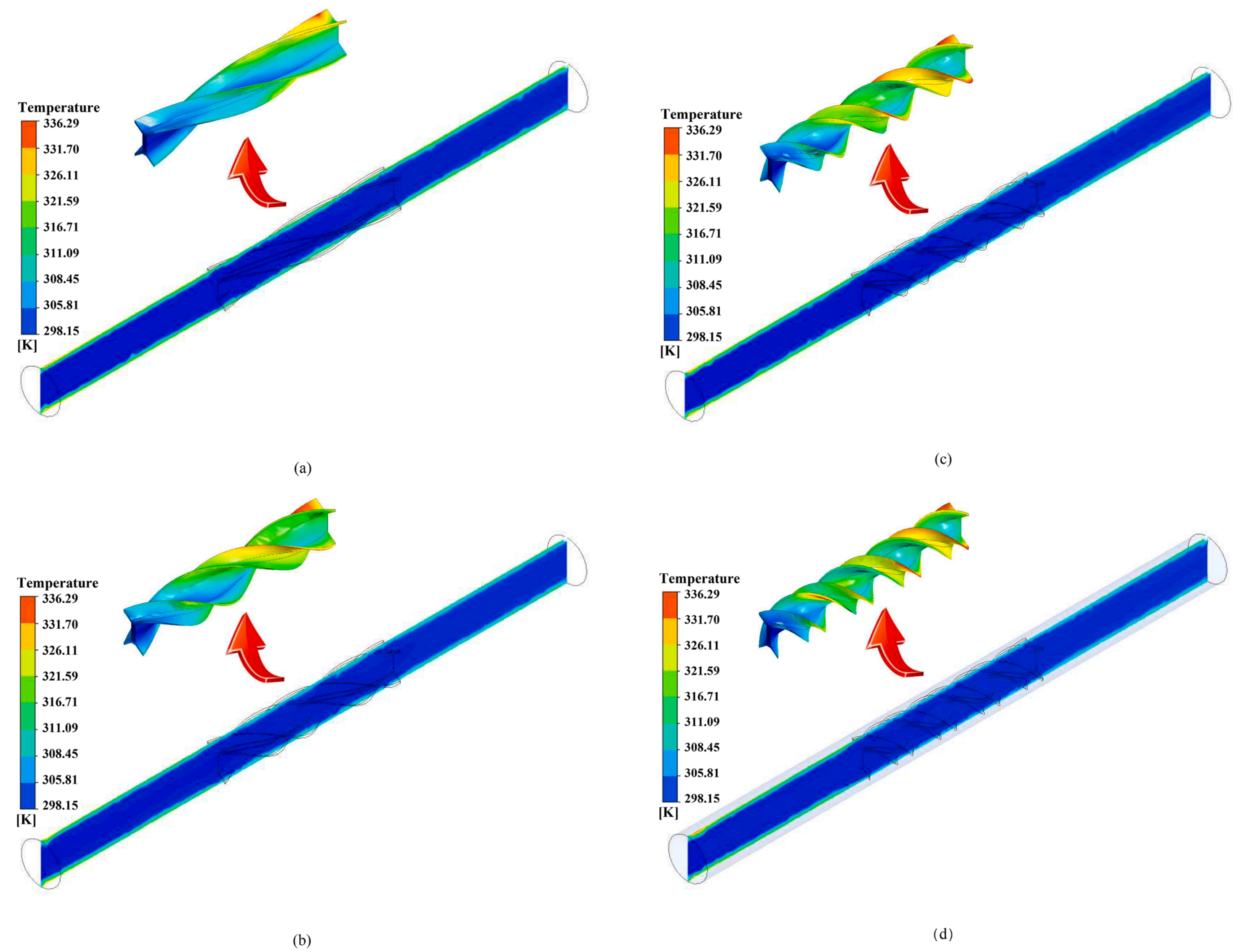

Fig. 7. Temperature contours for two −phasehybridnanofluid with φ = 3% and Re = 36000 are shown in Fig. 6 for (a) PR = 1, (b) PR = 2, (c) PR = 3, and (d) PR = 4.

and inlet and outlet is 250 mm. In this study, in order to model radiation, FLUENT software and surface-to-surface radiation model are used. The SST $k-\omega$ turbulence model is employed which means that the flow conforms to turbulent.

As reported in Table 1, SWCNT −Cu/water is used in this study.

In order to numerically simulate the SWCNT-Cu/water nanofluid flow inside the SC, the two-phase mixed method is used. The governing equations are as follows:

Continuity equation:

$$\frac{\partial}{\partial x_i}(\rho u_i) = 0 \tag{1}$$

Momentum equation:

$$\frac{\partial}{\partial x_i}(\rho u_i u_j) = -\frac{\partial p}{\partial x_i} + \frac{\partial \tau_{ij}}{\partial x_j} + \rho g_i \tag{2}$$

$$\tau_{ij} = \frac{\mu^* \partial u_i}{\partial x_j} \tag{3}$$

$$\mu^* = \mu + \mu_t \tag{4}$$

Energy equation:

$$\frac{\partial}{\partial x_i}(\rho c_p u_i T) = \frac{\partial}{\partial x_i}\left(\frac{\lambda^* \partial T}{\partial x_i}\right) \tag{5}$$

$$\lambda^* = \lambda + \lambda_t \tag{6}$$

$$\lambda_t = \frac{c_p \mu_t}{\sigma_t} \tag{7}$$

In this study, the k-ω turbulence model is used. This model has the capabilities of the k-ε model and also covers the weaknesses of that model. In fact, k-ω model has been used due to the higher accuracy and speed of convergence.

Similar to references of [48–50], the following turbulant formulations are utilized:

$$\frac{\partial}{\partial x_i}(\rho u_i k) = \frac{\partial}{\partial x_i}\left[\left(\mu + \frac{\mu_t}{\sigma_k}\right)\frac{\partial k}{\partial x_i}\right] + G_k - Y_k \tag{8}$$

$$\frac{\partial}{\partial x_i}(\rho u_i \omega) = \frac{\partial}{\partial x_i}\left[\left(\mu + \frac{\mu_t}{\sigma_\omega}\right)\frac{\partial k}{\partial x_i}\right] + G_\omega - Y_\omega + D_\omega \tag{9}$$

$$\mu_t = \frac{\rho k}{\omega}\frac{1}{\max\left\{\frac{1}{\alpha^*}, \frac{\Omega F_2}{a_1 \omega}\right\}} \tag{10}$$

$$\Omega = \sqrt{2\Omega_{ij}\Omega_{ij}} \tag{11}$$

where Ω_{ij} is the mean rate of rotation tensor and defined as follow [51]:

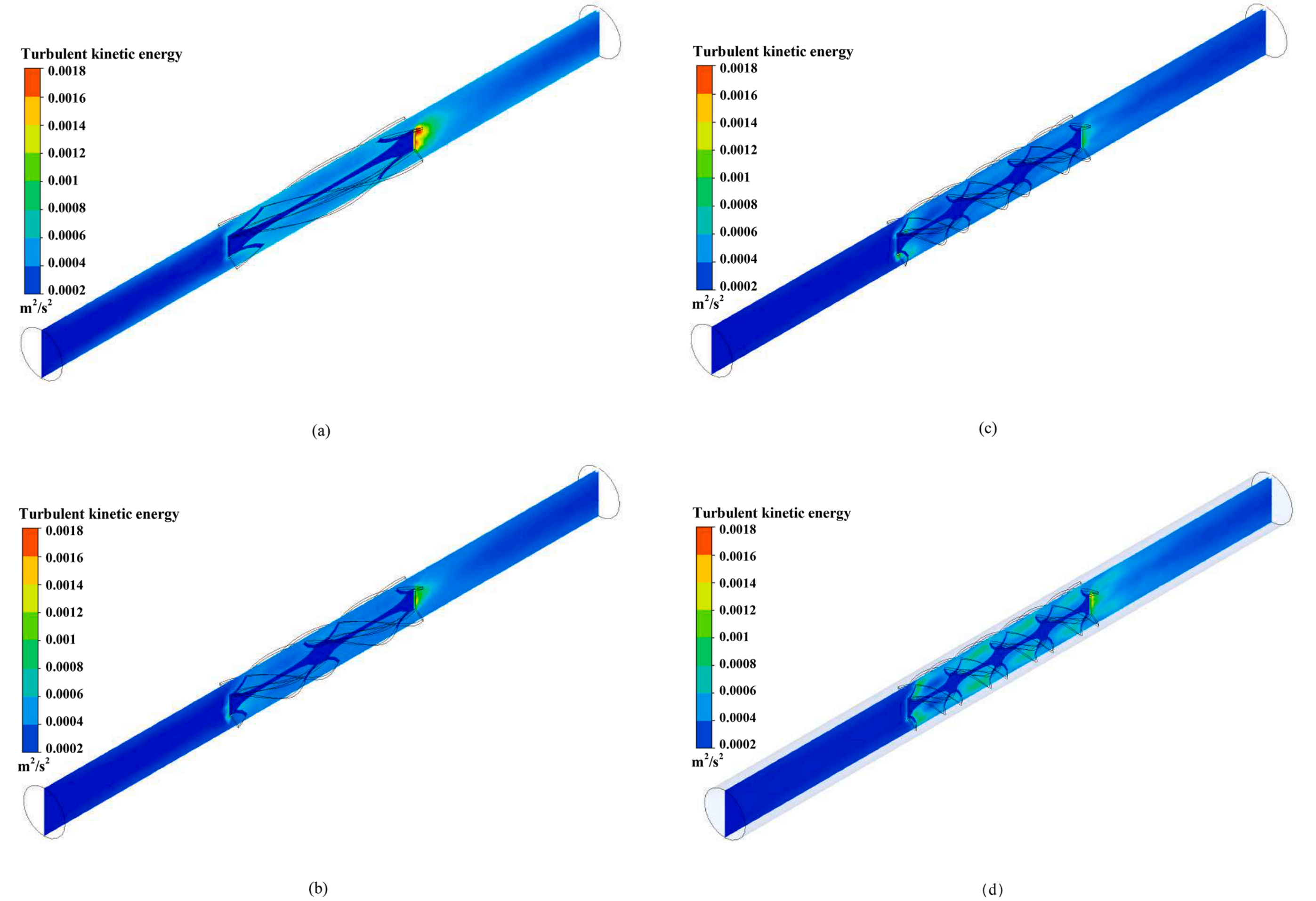

Fig. 8. Turbulence kinetic energy contours the temperature contours are plotted for two −phasehybridnanofluid with φ = 3% and Re = 36000 are shown in Fig. 6 for (a) PR = 1, (b) PR = 2, (c) PR = 3, and (d) PR = 4.

$$\Omega_{ij} = \frac{1}{2}\left(\frac{\partial u_i}{\partial x_j} - \frac{\partial u_j}{\partial x_i}\right) \tag{12}$$

The other notations in Eqs. 8–10 are defined as follows [50]:

$$\sigma_k = \frac{1}{\frac{F_1}{\sigma_{k,1}} + \frac{1-F_1}{\sigma_{k,2}}} \tag{13}$$

$$\sigma_\omega = \frac{1}{\frac{F_1}{\sigma_{\omega,1}} + \frac{1-F_1}{\sigma_{\omega,2}}} \tag{14}$$

$$F_1 = \tanh\left(\Phi_1^4\right) \tag{15}$$

$$F_2 = \tanh\left(\Phi_2^2\right) \tag{16}$$

$$\Phi_1 = \min\left\{\max\left\{\frac{\sqrt{k}}{0.09\omega y}, \frac{500\mu}{\rho y^2 \omega}\right\}, \frac{4\rho k}{\sigma_{\omega,2} D_\omega^+ y^2}\right\} \tag{17}$$

$$\Phi_2 = \max\left\{\frac{2\sqrt{k}}{0.09\omega y}, \frac{500\mu}{\rho y^2 \omega}\right\} \tag{18}$$

$$D_\omega^+ = \max\left\{\frac{2\rho}{\omega\rho_{\omega,2}} \frac{\partial k}{\partial x_i} \frac{\partial \omega}{\partial x_i}, 10^{-20}\right\} \tag{19}$$

$$\alpha^* = \alpha_\infty^* \left(\frac{\alpha_0^* + \frac{Re_t}{R_k}}{1 + \frac{Re_t}{R_k}}\right), \alpha_0^* = \frac{\beta_i}{3}, Re_t = \frac{\rho k}{\mu\omega}, \beta_i = F_1\beta_{i,1} + (1 - F_1)\beta_{i,2} \tag{20}$$

$$G_k = \tau_{t,ij}\frac{\partial u_i}{\partial x_j}, \tau_{t,ij} = \mu_t\left(\frac{\partial u_i}{\partial x_j} + \frac{\partial u_j}{\partial x_i}\right) - \frac{2}{3}\rho k \delta_{ij} \tag{21}$$

$$Y_k = \rho\beta^* k\omega, G_\omega = \frac{\rho\alpha}{\mu_t} G_k, Y_\infty = \rho\beta_i\omega^2 \tag{22}$$

$$\alpha = \frac{\alpha_\infty}{\alpha^*} = \left(\frac{\alpha_0^* + \frac{Re_t}{R_k}}{1 + \frac{Re_t}{R_k}}\right), \alpha_\infty = F_1\alpha_{\infty,1} + (1 - F_1)\alpha_{\infty,2} \tag{23}$$

$$\alpha_{\infty,1} = \frac{\beta_{i,1}}{\beta_\infty^*} - \frac{\kappa^2}{\sigma_{\omega,1}\sqrt{\beta_\infty^*}}, \alpha_{\infty,2} = \frac{\beta_{i,2}}{\beta_\infty^*} - \frac{\kappa^2}{\sigma_{\omega,2}\sqrt{\beta_\infty^*}} \tag{24}$$

Finaaly, the energetic and exergetic efficiencies are fefined as follows [31]:

$$\eta_n = \frac{E_n}{I \bullet A} = \frac{p_{fo} \bullet Q_{in} \bullet \rho_{in} \bullet c_{p,in} \bullet \left(T_{fo,out} - T_{in}\right) + \left(1 - p_{fo}\right) Q_{in} \bullet \rho_{in} \bullet c_{p,in} \bullet \left(T_{fi,out} - T_{in}\right)}{6 \bullet 10^4 \bullet I \bullet A} \tag{25}$$

$$\eta_{ex} = \frac{\dot{Q}_{HTF} - \dot{m}_{HTF} c_{p,HTF} \ln\left(\frac{T_\infty}{T_{i,HTF}}\right)}{-\dot{Q}_{HTF} - \dot{m}_{CF} c_{p,CF} \ln\left(\frac{T_{o,CF}}{T_{i,CF}}\right) + VI\eta_P} \tag{26}$$

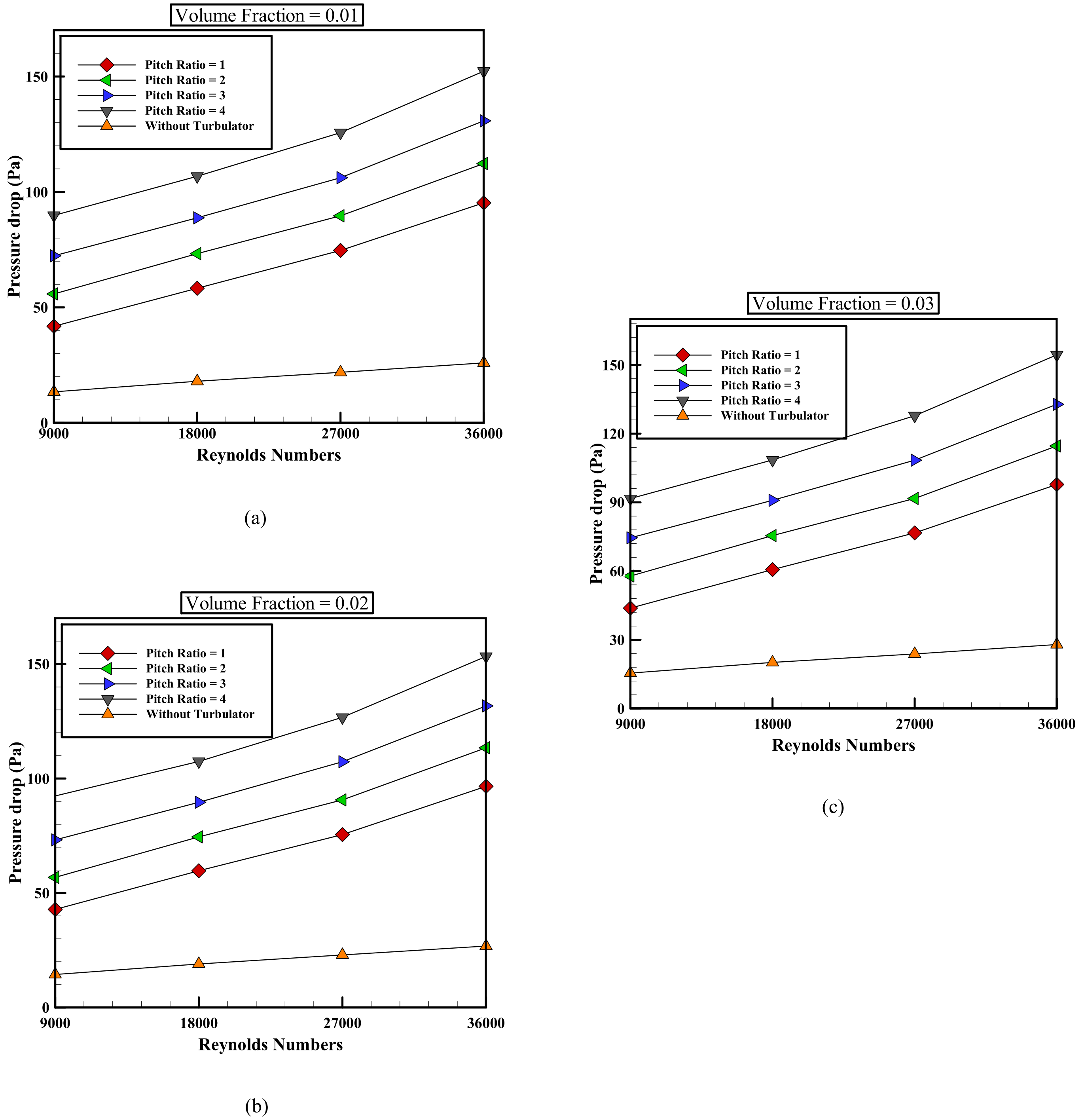

Fig. 9. Pressure drop in terms of Re in a SC equipped with a TT with different values of PR for (a) φ = 1%, (b) φ = 2%, and (c) φ = 3%.

Numerical modeling

In the present study, the effect of TT on THP, exergy and energy efficiency is examined using computational fluid dynamics and FLUENTs software. In order to solve the problem, the SOLIDWORKS software is used to design the geometry. Since Re changes from 9000 to 36000, the SST $k-\omega$ model is used to model turbulent flow. The solution is three-dimensional and steady. The SWCNT-Cu/water hybrid nanofluid is simulated using a two-phase mixed model. The first phase is the base fluid, and the second one is SWCNT and Cu nanoparticles. The coupled algorithm is used to couple the velocity and pressure equations. In order to spatially discretize gradients, the Green-Gauss Cell-Based model is employed.

Grid independence test

In order to study the grid independence, the $\overline{Nu}$ for SWCNT-Cu/water $two-phase hybrid nanofluid$ flow inside the SC with TT is calculated for different grid points (Fig. 3). The figure demonstrates that the grid with 2,436,268 elements is sufficient for the simulations. Further increase in the number of elements does not change the Nu. Therefore, it is possible to ensure the accuracy of the computational grid for the SC with a TT.

Verification

Verification of numerical results is performed based on the geometry

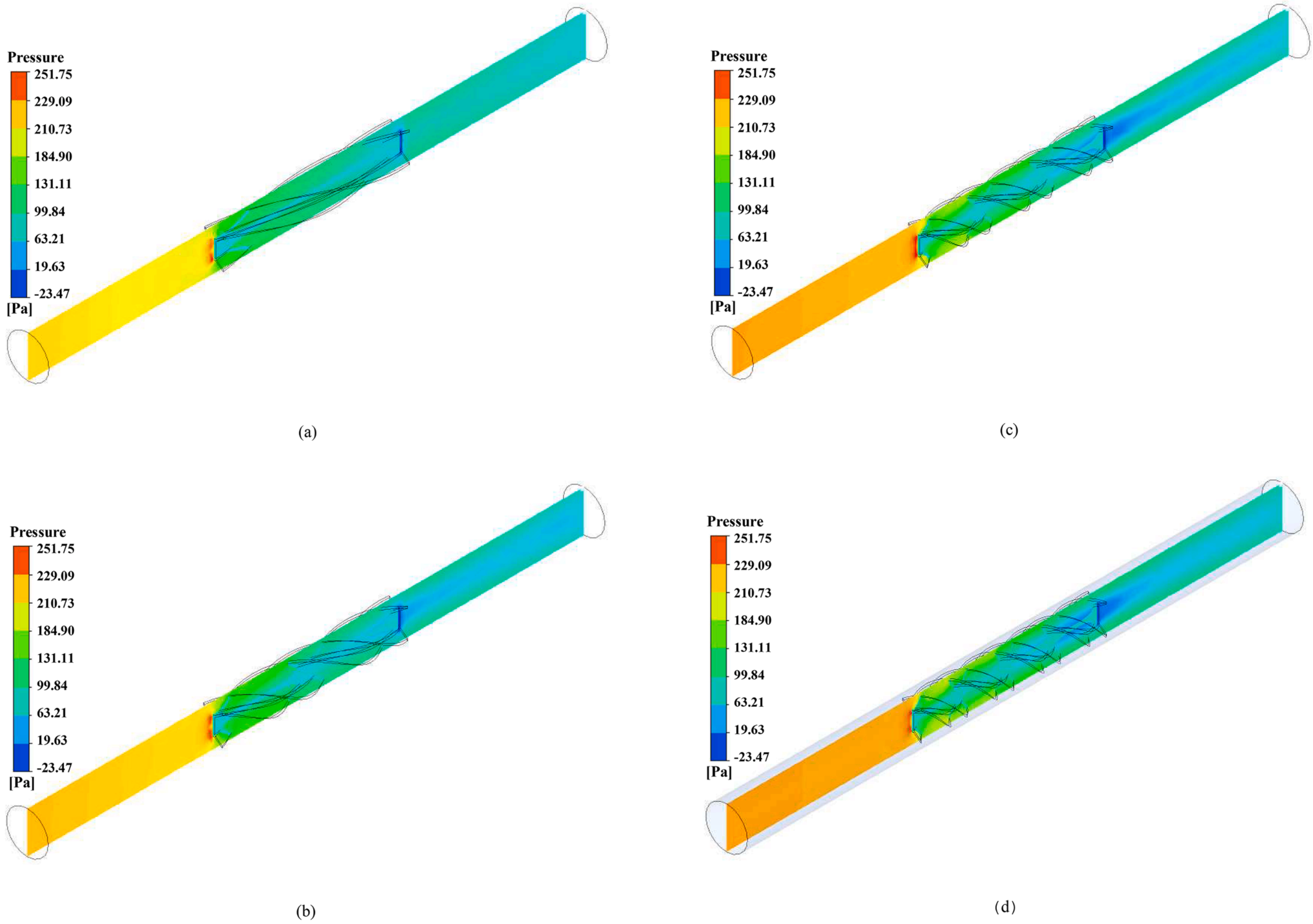

Fig. 10. Pressure contours for two −phasehybridnanofluid with φ = 3% and Re = 36000 for (a) PR = 1, (b) PR = 2, (c) PR = 3, and (d) PR = 4.

and boundary conditions of the study of He et al. [52]. The $\overline{Nu}$ is calculated and compared with their research (Fig. 4). The error between the values of the $\overline{Nu}$ obtained from the present simulations and the results of He et al. [52] is about 5.23%, indicating that the accuracy of the modeling results is ensured.

Results and discussion

In this section, the results of the present numerical simulations are presented. The effect of different values of PR of the TT on the $\overline{Nu}$, pressure drop, THP, and exergy and energy efficiency is investigated. Also, the counters of velocity, temperature, pressure, and streamlines inside the SC are provided for PR = 1, 2, 3, and 4, φ = 3%, and Re = 36000.

Effect of pitch ratio on $\overline{Nu}$

Figure 5 shows the variations of the $\overline{Nu}$ versus Re in a SC equipped with a TT with different values of PR for (a) φ = 1%, (b) φ = 2%, and (c) φ = 3%. According to the results, the $\overline{Nu}$ has an increasing trend with the φ and Re. For example, at Re = 36000, an increment in the PR enhances HT. Increasing the PR value has caused more fluctuation in the fluid flow, resulting in increased heat exchange, and therefore the average Nusselt number increases with increasing PR. For φ = 1% and Re = 36,000, the TT with PR = 4 intensifies the $\overline{Nu}$ by 71.45% compared to the SC without turbulator. At φ = 2% and Re = 36,000, the TT with PR = 4 enhances the $\overline{Nu}$ by 73.11% compared to the SC without turbulator. At φ = 3% and Re = 36,000, the TT with PR = 4 increases the average $\overline{Nu}$ by 74.95% compared to the SC without turbulator. With the use of turbulator, turbulence and oscillation in the flow increases and as a result, heat exchange between particles intensifies; thus, the average Nusselt number enhances.

Contours of velocity for two −phasehybridnanofluid with φ = 3% and Re = 36000 are shown in Fig. 6 for (a) PR = 1, (b) PR = 2, (c) PR = 3, and (d) PR = 4. As can be seen in the figures, the velocity of the SWCNT-Cu/water nanofluid is zero close to the wall and has its maximum value in the middle of the SC. Also, the use of a TT causes the mixing and disturbance to be created in the viscous sublayer. Therefore, the vortices are formed and enhance the thermal performance of the SC.

Figure 7 demonstrates the temperature contours for two −phasehybridnanofluid with φ = 3% and Re = 36000 are shown in Fig. 6 for (a) PR = 1, (b) PR = 2, (c) PR = 3, and (d) PR = 4. As can be seen, an increment in the PR of the TT causes the temperature at the turbulator surface to rise.

In Fig. 8, turbulent kinetic energy contours the temperature contours are plotted two −phasehybridnanofluid with φ = 3% and Re = 36000 are shown in Fig. 6 for (a) PR = 1, (b) PR = 2, (c) PR = 3, and (d) PR = 4. Due to the oscillating nature of the turbulent flow and the type of geometry studied, the speed fluctuations behind the turbulator increase. Because kinetic energy is caused by speed fluctuations, the amount of kinetic energy increases in this area.

Effect of pitch ratio on pressure drop

Figure 9 demonstrates the pressure drop in terms of Re in a SC

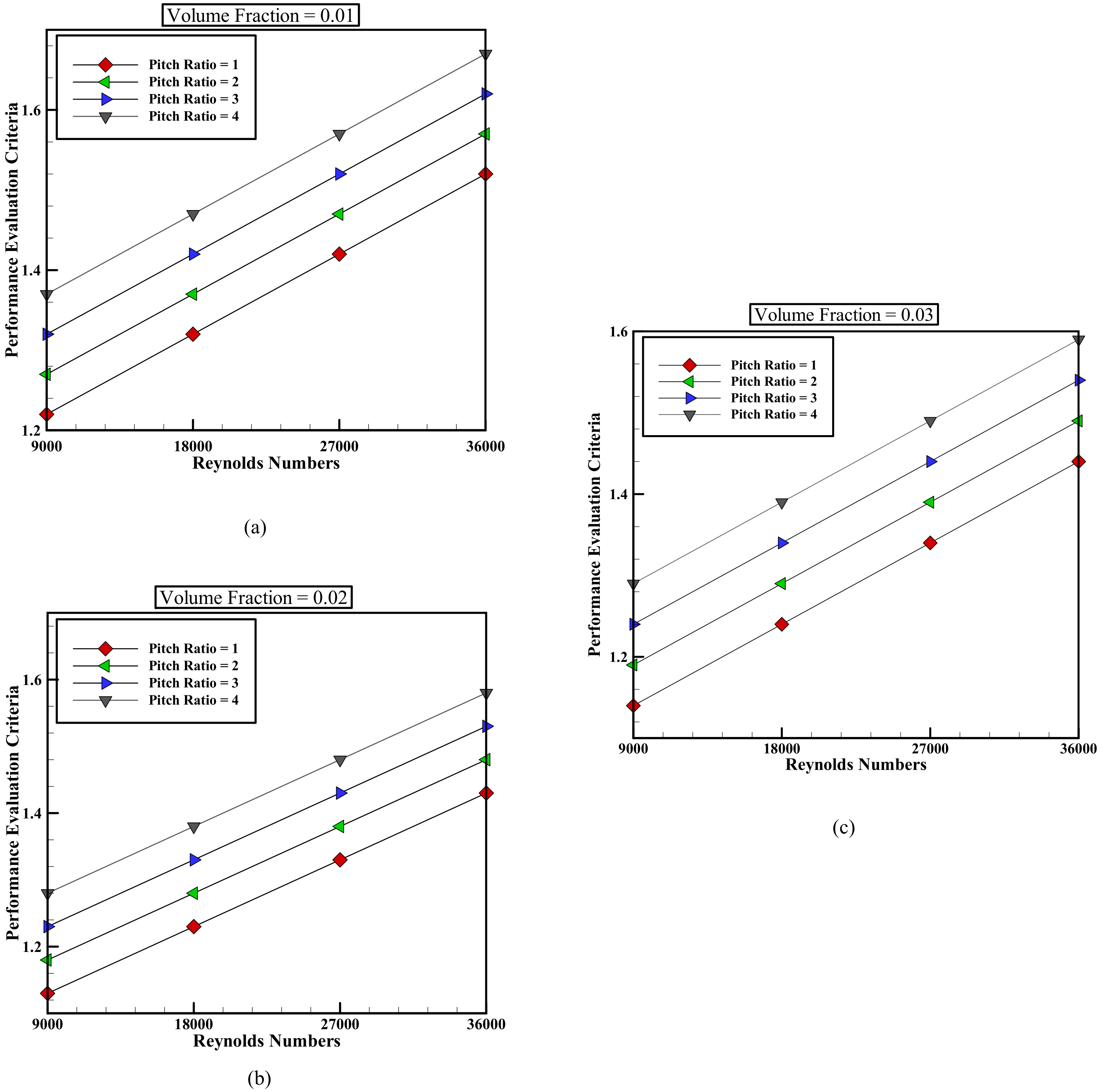

Fig. 11. Variations of THP in terms of Re for a SC equipped with a TT with different values of PR and (a) φ = 1%, (b) φ = 2%, and (c) φ = 3%.

equipped with a TT with different values of PR for (a) φ = 1%, (b) φ = 2%, and (c) φ = 3%. The pressure drop in the solar culture is an ascending function of the volume fraction of nanoparticles and Re. Increasing the volume fraction of nanoparticles intensifies the viscosity of hybrid nanofluid and as a result the amount of shear stresses rises. Also, an increment in the PR of the TT has a significant effect on pressure drop. As the PR value increases, the curvature in the turbulator rises and as a result, the flow lines become more curved. This event leads to more intense velocity gradients and augmented friction. This leads to an intensification in pressure drop.

At φ = 1% and Re = 36000, TTs with PR = 4 increase the pressure drop by 411.03% compared to the SC without turbulator. At φ = 2% and Re = 36,000, TTs with PR = 4 intensifies the pressure drop by 415.78% compared to the SC without turbulator. At φ = 3% and Re = 36,000, TTs with PR = 4 increase the pressure drop by 429.31% compared to the SC without turbulator.

The pressure contours are shown in Fig. 10 for two −phasehybridnanofluid with φ = 3% and Re = 36000 for (a) PR = 1, (b) PR = 2, (c) PR = 3, and (d) PR = 4. As can be seen, the accumulation of SWCNT-Cu/water two −phasehybridnanofluid flow is enhanced during the initial contact with the turbulator by intensifying the PR of the TT. Therefore, it can be concluded that an increment in the PR enhances the pressure drop.

Effect of pitch ratio on THP

Variations of THP in terms of Re are shown in Fig. 11 for a SC equipped with a TT with different values of PR and (a) φ = 1%, (b) φ =

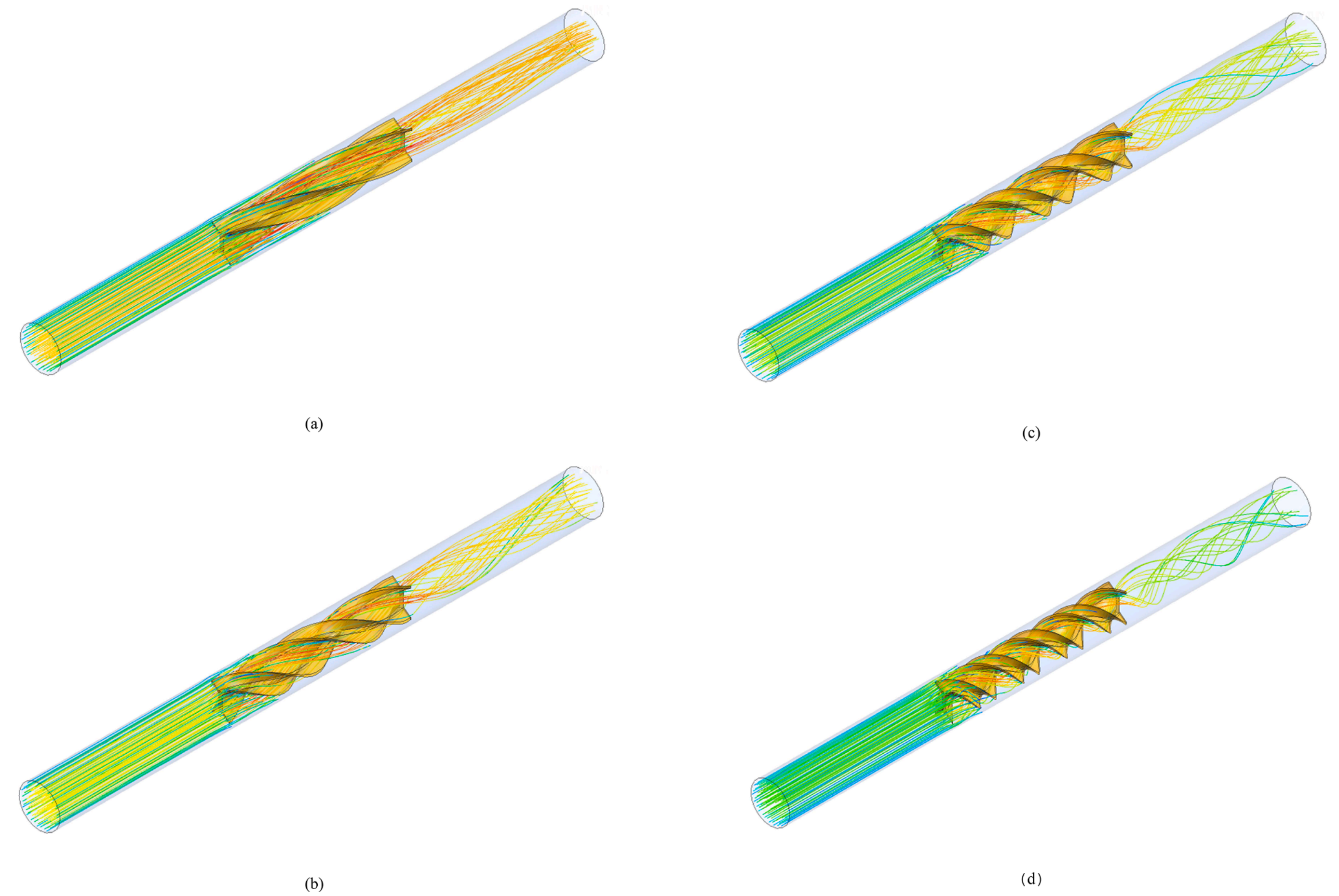

Fig. 12. Streamline contours for two −phasehybridnanofluid with φ = 3% and Re = 36000 for (a) PR = 1, (b) PR = 2, (c) PR = 3, and (d) PR = 4.

2%, and (c) φ = 3%. As can be seen, for all cases, the value of the THP is greater than 1. Therefore, the addition of a TT and an enhancement in its PR improve the THP. As the volume fraction of nanoparticles intensify, both the Nusselt number and the pressure drop augment. This augmentation is greater in the average Nusselt number compared to that in pressure drop. As a result, as the volume fraction of nanoparticles rises, the amount of PEC enahnces.

Streamline contours are shown in Fig. 12 for two −phasehybridnanofluid with φ = 3% and Re = 36000 for (a) PR = 1, (b) PR = 2, (c) PR = 3, and (d) PR = 4. As can be seen, the density of the streamlines enhances with the PR.

Effect of pitch ratio on energy efficiency

Figure 13 illustrates the energy efficiency in terms of Re for a SC equipped with a TT with different volume fractions and (a) PR = 1, (b) PR = 2, (c) PR = 3, and (d) PR = 4. For all cases, the energy efficiency is an ascending function of the pitch ratio of the TT. In a SC with a TT with a pitch ratio of 1 and φ = 3%, the amount of energy efficiency is enhanced by 35.81% by increasing the Re from 7000 to 28000.

In a SC with a TT with PR = 2 and φ = 3%, the amount of energy efficiency intensifies by 37.90% by enhancing the Re from 7000 to 28000. In a SC with a TT with PR = 3 and φ = 3%, the amount of energy efficiency is enhanced by 39.07% by intensifying the Re from 7000 to 28000. In a SC with a TT with PR = 4 and φ = 3%, the amount of energy efficiency is enhanced by 41.75% by increasing the Re from 7000 to 28000.

Effect of pitch ratio on exergy efficiency

Exergy efficiency as a function of Re is presented in Fig. 14 for a SC equipped with a TT with different values of φ and (a) PR = 1, (b) PR = 2, (c) PR = 3, and (d) PR = 4. The exergy efficiency is an ascending function of Re and φ. In a SC with a TT with PR = 1 and φ = 3%, the amount of exergy efficiency is enhanced by 33.09% by increasing the Re from 9000 to 36000. In a SC with a TT with PR = 2 and φ = 3%, the amount of exergy efficiency enhances by 32.32% by intensifying the Re from 9000 to 36000. In a SC with a TT with PR = 3 and φ = 3%, the amount of exergy efficiency is increased by 30.11% by enhancing the Re from 9000 to 36000. In a SC with a TT with PR = 4 and φ = 3%, the amount of exergy efficiency enhances by 30.67% by increasing the Re from 9000 to 36000.

Conclusions

In the present numerical study, the impact of TT in a SC on energy and exergy efficiencies and THP of SWCNT-Cu/water hybrid nanofluid was evaluated. The study was performed for Re in the range of 9000 to 36000, φ = 1 to 3%, and PR = 1, 2, 3, and 4. Based on the results obtained from the numerical study, it can be concluded:

The pressure drop and the $\overline{Nu}$ enhance by intensifying the PR of the TT.

- At φ = 3% and Re = 36,000, the placement of TTs with PR = 4 enhances the $\overline{Nu}$ by 74.95% compared to the SC without turbulator.

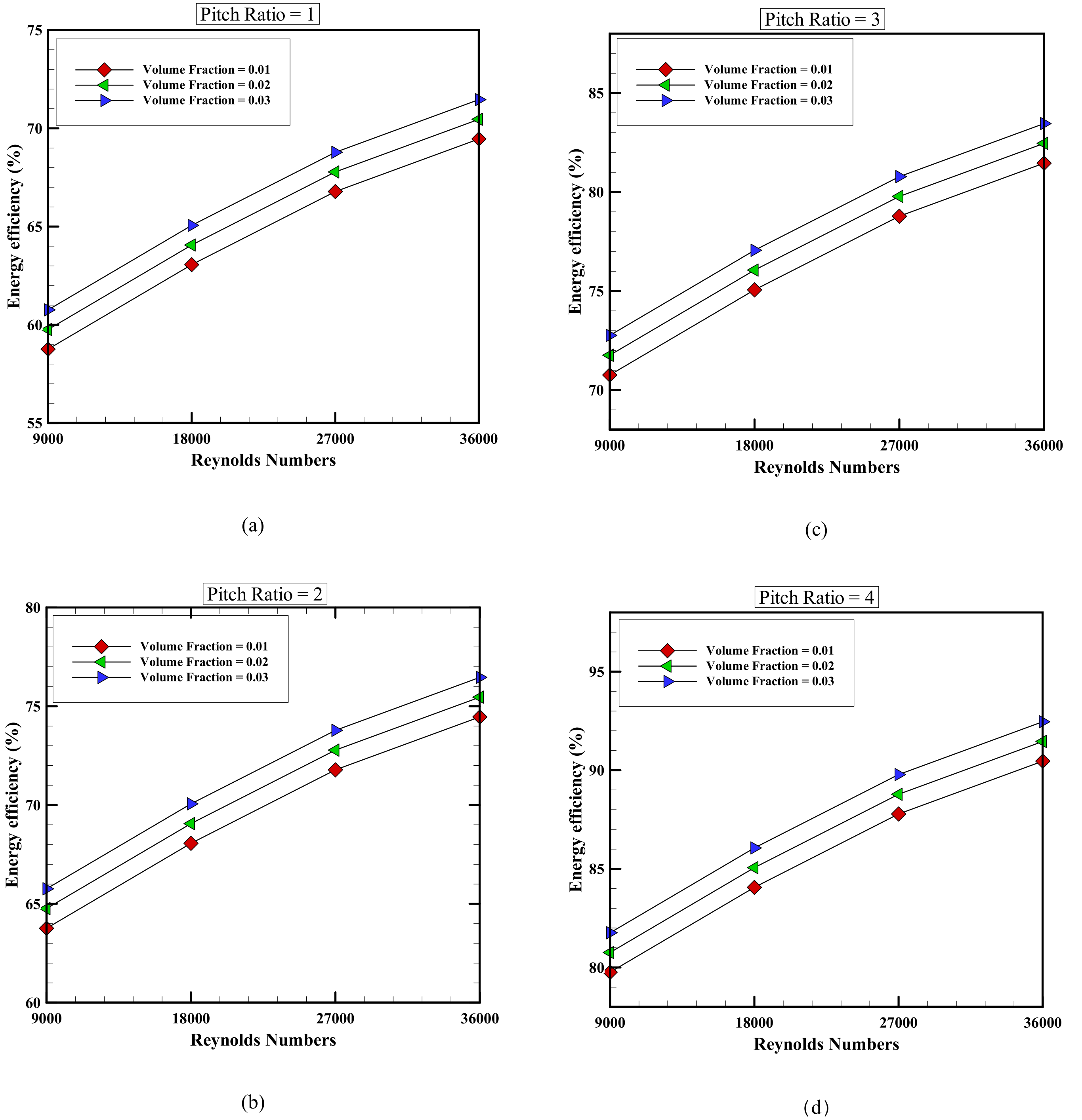

Fig. 13. Energy efficiency in terms of Re for a SC equipped with a TT with different values of φ and (a) PR = 1, (b) PR = 2, (c) PR = 3, and (d) PR = 4.

- For all cases, the values of the THP are greater than 1. Therefore, it can be concluded that the addition of a TT and an increment in its pitch ratio improve the THP.
- For all cases, the energy efficiency is an ascending function of the PR.
- In a SC with a TT with PR = 4 and φ = 3%, the amount of energy efficiency is enhanced by 41.75% by increasing the Reynolds number from 7000 to 28000.
- Exergy efficiency is an ascending function of Re and φ.
- In a SC with a TT with PR = 1 and φ = 3%, the amount of exergy efficiency intensifies by 33.09% by enhancing the Re from 9000 to 36000.

CRediT authorship contribution statement

Muhammad Ibrahim: Funding acquisition, Writing – original draft. **Awatef Abidi:** Formal analysis, Writing – original draft. **Ebrahem A. Algehyne:** Writing – original draft. **Tareq Saeed:** Writing – original draft. **Goshtasp Cheraghian:** Conceptualization, Writing – review & editing. **Mohsen Sharifpur:** Conceptualization.

Declaration of Competing Interest

The authors declare that they have no known competing financial interests or personal relationships that could have appeared to influence the work reported in this paper.

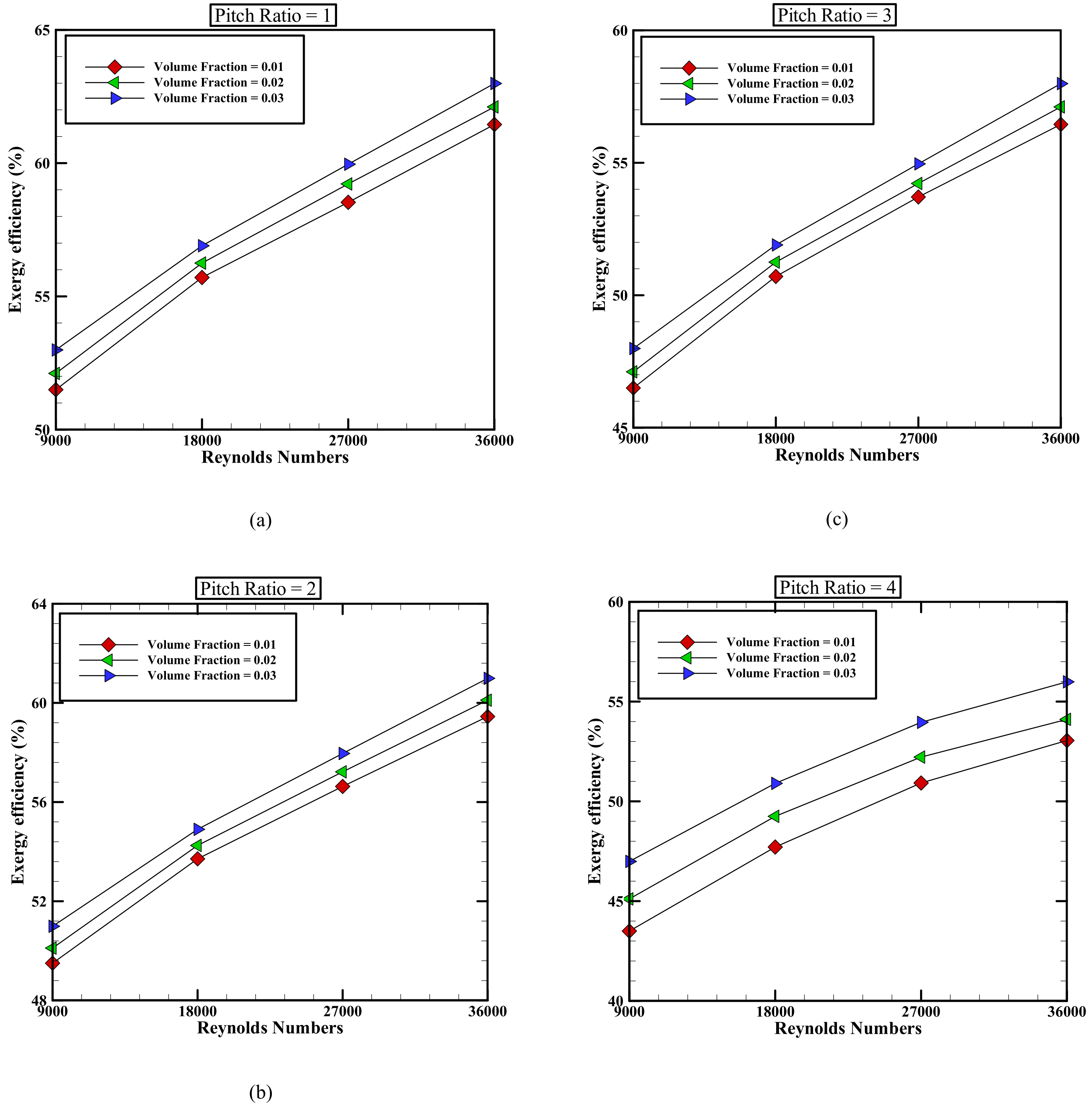

Fig. 14. Exergy efficiency as a function of Re for a SC equipped with a TT with different values of φ and (a) PR = 1, (b) PR = 2, (c) PR = 3, and (d) PR = 4.

Acknowledgments

The second author extends her appreciation to the Deanship of Scientific Research at King Khalid University, Abha, Saudi Arabia for funding this work through the Research Group under grant number (R.G.P.1/329/42)

References

[1] Ghazvini M, Pourkiaei S, Pourfayaz F. Thermo-economic assessment and optimization of actual heat engine performance by implemention of NSGA II. Renew Energy Res Appl 2020;1:235–45.

[2] Kaushal R, Kumar R. Heat transfer enhancement using augmented tubes for desalination using Fuzzy-TOPSIS approach. Renew Energy Res Appl 2020;1:19–26.

[3] Parsa SM, Rahbar A, Javadi Y D, Koleini MH, Afrand M, Amidpour M. Energy-matrices, exergy, economic, environmental, exergoeconomic, enviroeconomic, and heat transfer (6E/HT) analysis of two passive/active solar still water desalination nearly 4000m: altitude concept. J Cleaner Prod 2020;261:121243. https://doi.org/10.1016/j.jclepro.2020.121243.

[4] Sultan SM, Tso C, E.E. M N. A case study on effect of inclination angle on performance of photovoltaic solar thermal collector in forced fluid mode. Renew Energy Res Appl. 2020;1:187–96.

[5] Parsa SM, Yazdani A, Dhahad H, Alawee WH, Hesabi S, Norozpour F, et al. Effect of Ag, Au, TiO2 metallic/metal oxide nanoparticles in double-slope solar stills via thermodynamic and environmental analysis. J Cleaner Prod 2021;311:127689. https://doi.org/10.1016/j.jclepro.2021.127689.

[6] Mohamed H, Bani-Hani E, EL Haj Assad M. Thermal analysis of organic rankine cycle using different organic fluids. Renew Energy Res Appl 2020;1:115–21.

[7] Naseri A, Fazlikhani M, Sadeghzadeh M, Naeimi A, Bidi M, Tabatabaei SH. Thermodynamic and exergy analyses of a novel solar-powered CO2 transcritical

power cycle with recovery of cryogenic LNG using stirling engines. Renew Energy Res Appl 2020;1:175–85.
[8] Kalbasi R, Jahangiri M, Mosavi A, Jalaladdin Hosseini Dehshiri S, Shahabaddin Hosseini Dehshiri S, Ebrahimi S, et al. Finding the best station in Belgium to use residential-scale solar heating, One-year dynamic simulation with considering all system losses: economic analysis of using ETSW. Sustain Energy Technol Assess 2021;45:101097. https://doi.org/10.1016/j.seta.2021.101097.
[9] Menni Y, Ghazvini M, Ameur H, Ahmadi MH, Sharifpur M, Sadeghzadeh M. Numerical calculations of the thermal-aerodynamic characteristics in a solar duct with multiple V-baffles. Eng Appl Comput Fluid Mech 2020;14(1):1173–97.
[10] Menni Y, Ghazvini M, Ameur H, Kim M, Ahmadi MH, Sharifpur M. Combination of baffling technique and high-thermal conductivity fluids to enhance the overall performances of solar channels. Eng Comput 2020:1–22.
[11] Shahsavar Goldanlou A, Kalbasi R, Afrand M. Energy usage reduction in an air handling unit by incorporating two heat recovery units. J Build Eng 2020;32:101545.
[12] Liu W, Kalbasi R, Afrand M. Solutions for enhancement of energy and exergy efficiencies in air handling units. J Cleaner Prod 2020;257:120565.
[13] Karimipour A, Bahrami D, Kalbasi R, Marjani A. Diminishing vortex intensity and improving heat transfer by applying magnetic field on an injectable slip microchannel containing FMWNT/water nanofluid. J Therm Anal Calorim 2021;144:2235–46.
[14] Nguyen Q, Bahrami D, Kalbasi R, Bach QV. Nanofluid flow through microchannel with a triangular corrugated wall: heat transfer enhancement against entropy generation intensification. Math Methods Appl Sci. n/a 2020.
[15] Nguyen Q, Bahrami D, Kalbasi R, Karimipour A. Functionalized multi-walled carbon nano tubes nanoparticles dispersed in water through an magneto hydro dynamic nonsmooth duct equipped with sinusoidal-wavy wall: diminishing vortex intensity via nonlinear Navier–Stokes equations. Math Methods Appl Sci. n/a 2020.
[16] Ahmadi AA, Arabbeiki M, Ali HM, Goodarzi M, Safaei MR. Configuration and optimization of a minichannel using water–alumina nanofluid by non-dominated sorting genetic algorithm and response surface method. Nanomaterials 2020;10:901.
[17] Ahmadi MH, Mohseni-Gharyehsafa B, Ghazvini M, Goodarzi M, Jilte RD, Kumar R. Comparing various machine learning approaches in modeling the dynamic viscosity of CuO/water nanofluid. J Therm Anal Calorim 2020;139:2585–99.
[18] Giwa SO, Sharifpur M, Ahmadi MH, Meyer JP. Magnetohydrodynamic convection behaviours of nanofluids in non-square enclosures: a comprehensive review. Math Methods Appl Sci 2020.
[19] Giwa SO, Sharifpur M, Ahmadi MH, Meyer JP. A review of magnetic field influence on natural convection heat transfer performance of nanofluids in square cavities. J Therm Anal Calorim 2021;145(5):2581–623.
[20] Jahangir MH, Ghazvini M, Pourfayaz F, Ahmadi MH, Sharifpur M, Meyer JP. Numerical investigation into mutual effects of soil thermal and isothermal properties on heat and moisture transfer in unsaturated soil applied as thermal storage system. Num. Heat Transf Part A: Appl 2018;73(7):466–81.
[21] Usmani R, Hussain F, Khan SA, Khan NA, Khan U, Husain S. Numerical investigation on natural convection of hybrid nanofluid Al2O3 – MWCNT/water inside a vertical annulus. IOP Conf Ser: Mater Sci Eng 2021;1146:012018.
[22] Husain S, Khan SA, Siddiqui MA. Wall boiling of Al2O3-water nanofluid: effect of nanoparticle concentration. Prog Nucl Energy 2021;133:103614. https://doi.org/10.1016/j.pnucene.2020.103614.
[23] Khan SA, Altamush Siddiqui M, Husain S. Numerical studies on thermally induced flow of nanofluid in a vertical annulus. In: Yadav S, Singh DB, Arora PK, Kumar H, editors. Proceedings of international conference in mechanical and energy technology: ICMET 2019, India. Singapore: Springer Singapore; 2020, p. 87–100.
[24] Rostami S, Kalbasi R, Talebkeikhah M, Goldanlou AS. Improving the thermal conductivity of ethylene glycol by addition of hybrid nano-materials containing multi-walled carbon nanotubes and titanium dioxide: applicable for cooling and heating. J Therm Anal Calorim 2021;143:1701–12.
[25] Wei H, Afrand M, Kalbasi R, Ali HM, Heidarshenas B, Rostami S. The effect of tungsten trioxide nanoparticles on the thermal conductivity of ethylene glycol under different sonication durations: an experimental examination. Powder Technol 2020;374:462–9.
[26] Yan S-R, Kalbasi R, Karimipour A, Afrand M. Improving the thermal conductivity of paraffin by incorporating MWCNTs nanoparticles. J Therm Anal Calorim 2021;145(5):2809–16.
[27] Motamedi M, Eskandari M, Yeganeh M. Effect of straight and wavy carbon nanotube on the reinforcement modulus in nonlinear elastic matrix nanocomposites. Mater Des 2012;34:603–8.
[28] Motamedi M, Mashhadi MM, Rastgoo A. Vibration behavior and mechanical properties of carbon nanotube junction. J Comput Theor Nanosci 2013;10:1033–7.
[29] Motamedi M, Naghdi AH, Jalali SK. Effect of temperature on properties of aluminum/single-walled carbon nanotube nanocomposite by molecular dynamics simulation. Proc Inst Mech Eng C J Mech Eng Sci 2020;234(2):635–42.
[30] Giwa SO, Sharifpur M, Ahmadi MH, Sohel Murshed SM, Meyer JP. Experimental investigation on stability, viscosity, and electrical conductivity of water-based hybrid nanofluid of MWCNT-Fe2O3. Nanomaterials 2021;11:136.
[31] Hong K, Yang Y, Rashidi S, Guan Y, Xiong Q. Numerical simulations of a Cu–water nanofluid-based parabolic-trough solar collector. J Therm Anal Calorim 2021;143:4183–95.
[32] Alimoradi A, Fatahi M, Rehman S, Khoshvaght-Aliabadi M, Hassani S. Effects of transversely twisted-turbulators on heat transfer and pressure drop of a channel with uniform wall heat flux. Chem Eng Process-Process Intensif 2020;154:108027.
[33] Dezfulizadeh A, Aghaei A, Joshaghani AH, Najafizadeh MM. Exergy efficiency of a novel heat exchanger under MHD effects filled with water-based Cu–SiO 2-MWCNT ternary hybrid nanofluid based on empirical data. J Therm Anal Calorim 2021:1–24.
[34] Wu S-Y, Luo J-G, Xiao L, Chen Z-L. Effect of different errors on deformation and thermal stress of absorber tube in solar parabolic trough collector. Int J Mech Sci 2020;188:105969.
[35] Ebrahimpour Z, Sheikholeslami M. Investigation of nanofluid convective flow through a solar system equipped with mirrors. J Mol Liq 2021;335:116198. https://doi.org/10.1016/j.molliq.2021.116198.
[36] Shanazari E, Kalbasi R. Improving performance of an inverted absorber multi-effect solar still by applying exergy analysis. Appl Therm Eng 2018;143:1–10.
[37] Li Z, Du C, Ahmadi D, Kalbasi R, Rostami S. Numerical modeling of a hybrid PCM-based wall for energy usage reduction in the warmest and coldest months. J Therm Anal Calorim 2021;144(5):1985–98.
[38] Nazir MS, Ghasemi A, Dezfulizadeh A, Abdalla AN. Numerical simulation of the performance of a novel parabolic solar receiver filled with nanofluid. J Therm Anal Calorim 2021;144:2653–64.
[39] Akbarzadeh S, Valipour MS. Energy and exergy analysis of a parabolic trough collector using helically corrugated absorber tube. Renew Energy 2020;155:735–47.
[40] Ma Y, Jamiatia M, Aghaei A, Sepehrirad M, Dezfulizadeh A, Afrand M. Effect of differentially heated tubes on natural convection heat transfer in a space between two adiabatic horizontal concentric cylinders using nano-fluid. Int J Mech Sci 2019;163:105148.
[41] Chang C, Xu C, Wu Z, Li X, Zhang Q, Wang Z. Heat transfer enhancement and performance of solar thermal absorber tubes with circumferentially non-uniform heat flux. Energy Procedia 2015;69:320–7.
[42] Mashayekhi R, Khodabandeh E, Bahiraei M, Bahrami L, Toghraie D, Akbari OA. Application of a novel conical strip insert to improve the efficacy of water–Ag nanofluid for utilization in thermal systems: a two-phase simulation. Energy Convers Manage 2017;151:573–86.
[43] Siavashi M, Bahrami HRT, Saffari H. Numerical investigation of porous rib arrangement on heat transfer and entropy generation of nanofluid flow in an annulus using a two-phase mixture model. Num Heat Transf Part A: Appl 2017;71(12):1251–73.
[44] Goldanlou AS, Sepehrirad M, Dezfulizadeh A, Golzar A, Badri M, Rostami S. Effects of using ferromagnetic hybrid nanofluid in an evacuated sweep-shape solar receiver. J Therm Anal Calorim 2021;143:1623–36.
[45] Varzaneh AA, Toghraie D, Karimipour A. Comprehensive simulation of nanofluid flow and heat transfer in straight ribbed microtube using single-phase and two-phase models for choosing the best conditions. J Therm Anal Calorim 2020;139:701–20.
[46] Rostami S, Sepehrirad M, Dezfulizadeh A, Hussein AK, Shahsavar Goldanlou A, Shadloo MS. Exergy optimization of a solar collector in flat plate shape equipped with elliptical pipes filled with turbulent nanofluid flow: a study for thermal management. Water 2020;12:2294.
[47] Fadodun OG, Amosun AA, Okoli NL, Olaloye DO, Ogundeji JA, Durodola SS. Numerical investigation of entropy production in SWCNT/H 2 O nanofluid flowing through inwardly corrugated tube in turbulent flow regime. J Therm Anal Calorim 2021;144:1451–66.
[48] I. Ansys. Cfx-solver theory guide, Release 12.1 ed. 2009.
[49] Behzadmehr A, Saffar-Avval M, Galanis N. Prediction of turbulent forced convection of a nanofluid in a tube with uniform heat flux using a two phase approach. Int J Heat Fluid Flow 2007;28:211–9.
[50] Hejazian M, Moraveji MK, Beheshti A. Comparative study of Euler and mixture models for turbulent flow of Al2O3 nanofluid inside a horizontal tube. Int Commun Heat Mass Transf 2014;52:152–8.
[51] Göktepe S, Atalık K, Ertürk H. Comparison of single and two-phase models for nanofluid convection at the entrance of a uniformly heated tube. Int J Therm Sci 2014;80:83–92.
[52] He W, Toghraie D, Lotfipour A, Pourfattah F, Karimipour A, Afrand M. Effect of twisted-tape inserts and nanofluid on flow field and heat transfer characteristics in a tube. Int Commun Heat Mass Transf 2020;110:104440.
[53] Li Xin, Gui De, Zhao Zhangfei, Li Xinyu, Wu Xian, Hua Yawen, et al. Operation optimization of electrical-heating integrated energy system based on concentrating solar power plant hybridized with combined heat and power plant. J Clean Prod 2021;289:125712. https://doi.org/10.1016/j.jclepro.2020.125712.
[54] Wang Peng, Wang Su-Zhen, Kang Ya-Ru, Sun Zhong-Sen, Wang Xue-Dong, Meng Yu, et al. Cauliflower-shaped Bi_2O_3–ZnO heterojunction with superior sensing performance towards ethanol. J Alloys and Comp 2021;854:157152. https://doi.org/10.1016/j.jallcom.2020.157152.
[55] Wu Hao, Zhang Fujun, Zhang Zhenyu. Droplet breakup and coalescence of an internal-mixing twin-fluid spray. Physics of Fluids 2021;33:013317. https://doi.org/10.1063/5.0030777.
[56] Wang Xiaoming, Li Changhe, Zhang Yanbin, Said Zafar, Debnath Sujan, Sharma Shubham, et al. Influence of texture shape and arrangement on nanofluid minimum quantity lubrication turning. The International Journal of Advanced Manufacturing Technology 2021. https://doi.org/10.1007/s00170-021-08235-4. In press.